Oncogene (2004) 23, 1010–1013

www.nature.com/onc

Effects of Herceptin treatment on global gene expression patterns in *HER2*-amplified and nonamplified breast cancer cell lines

Päivikki Kauraniemi[1], Sampsa Hautaniemi[2], Reija Autio[2], Jaakko Astola[2], Outi Monni[3], Abdel Elkahloun[4] and Anne Kallioniemi*[,1]

[1]*Laboratory of Cancer Genetics, Institute of Medical Technology, University of Tampere and Tampere University Hospital, FIN-33520 Tampere, Finland;* [2]*Institute of Signal Processing, Tampere University of Technology, FIN-33101 Tampere, Finland;* [3]*Biomedicum Biochip Center, University of Helsinki, Biomedicum Helsinki, FIN-00290 Helsinki, Finland;* [4]*Cancer Genetics Branch, National Human Genome Research Institute, NIH, Bethesda, MD 20892, USA*

Herceptin is a humanized monoclonal antibody targeted against the extracellular domain of the *HER2* oncogene, which is amplified and overexpressed in 10–34% of breast cancers. Herceptin therapy provides effective treatment in *HER2*-positive metastatic breast cancer, although a favorable treatment response is not achieved in all cases. Here, we show that Herceptin treatment induces a dose-dependent growth reduction in breast cancer cell lines with *HER2* amplification, whereas nonamplified cell lines are practically resistant. Time-course analysis of global gene expression patterns in amplified and nonamplified cell lines indicated a major change in transcript levels between 24 and 48 h of Herceptin treatment. A step-wise gene selection algorithm revealed a set of 439 genes whose temporal expression profiles differed most between the amplified and nonamplified cell lines. The discriminatory power of these genes was confirmed by both hierarchical clustering and self-organizing map analyses. In the amplified cell lines, the Herceptin treatment induced the expression of several genes involved in RNA processing and DNA repair, while cell adhesion mediators and known oncogenes, such as *c-FOS* and *c-KIT*, were downregulated. These results provide additional clues to the downstream effects of blocking the *HER2* pathway in breast cancer and may provide new targets for more effective treatment.

Oncogene (2004) **23,** 1010–1013. doi:10.1038/sj.onc.1207200
Published online 1 December 2003

Keywords: *HER2*; herceptin; amplification; breast cancer; cDNA microarray

The *HER2* proto-oncogene encodes a 185 kDa transmembrane glycoprotein, which is one component of the four-member growth factor receptor family, including closely related EGFR, HER3, and HER4 proteins. The amplification and overexpression of HER2 is found in 10–34% of human breast cancers, and has been associated with poor clinical outcome in several studies (reviewed in Ross and Fletcher, 1999). Recently, targeted antibody-based therapy against HER2 protein was developed (Carter *et al*., 1992). The recombinant humanized monoclonal antibody Herceptin binds to the extracellular domain of the HER2 receptor with high affinity and disrupts various downstream signaling events leading ultimately to reduced cell growth (Molina *et al*., 2001; Yakes *et al*., 2002). Several studies have demonstrated the effectiveness of this new anticancer therapy against a subset of advanced breast tumors with HER2 overexpression, although for unknown reasons all tumors with HER2 activation do not respond favorably (Baselga *et al*., 1996; Cobleigh *et al*., 1999; Slamon *et al*., 2001; Vogel *et al*., 2002). In this study, we investigated the effects of Herceptin treatment on gene expression patterns in *HER2*-amplified and nonamplified breast cancer cell lines to elucidate the molecular consequences of blocking the *HER2* pathway.

Breast cancer cell lines BT-474, SK-BR-3, and ZR-75-30 previously shown to display high-level amplification and overexpression of HER2, MDA-453 harboring low-level amplification (2.8-fold relative to the chromosome 17 centromere) accompanied by only a modest increase in HER2 expression, as well as MCF7 and MDA-436 with neither amplification nor increased expression, were included in this study (Kauraniemi *et al*., 2001; Hyman *et al*., 2002). Cells were harvested at the exponential growth phase and plated on 96-well plates. After an initial growth period of 48 h (to achieve an at least 70% confluency) in recommended medium and culture conditions, Herceptin was added to the test cells at various concentrations (1, 10, 100, and 500 μg/ml). Antibody treatment was carried out for 72 h, followed by cell growth analysis. As expected, the cell lines with *HER2* amplification showed a clear reduction in growth after Herceptin treatment (Figure 1). This growth reduction was dose-dependent and already detectable with 1 μg/ml Herceptin. The most prominent effect was seen in SK-BR-3 cells that illustrated a 20% growth suppression with 1 μg/ml Herceptin and a 70% growth reduction with 500 μg/ml Herceptin (Figure 1). The *HER2* nonamplified cell lines showed negligible growth suppression with low doses of Herceptin, but

*Correspondence: A Kallioniemi; E-mail: anne.kallioniemi@uta.fi
Received 26 May 2003; revised 2 September 2003; accepted 10 September 2003

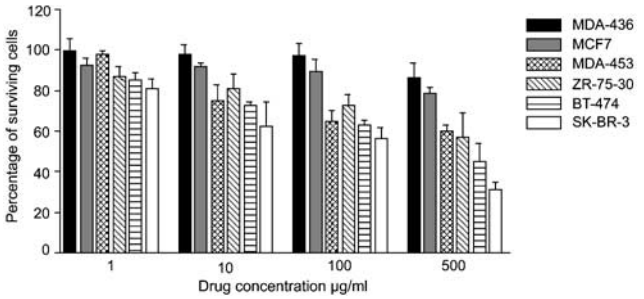

Figure 1 Herceptin treatment induced growth suppression in breast cancer cell lines. Breast cancer cell lines obtained from ATCC (Manassas, VA, USA) were grown under recommended culture conditions. Exponentially growing cells were harvested and plated on 96-well plates at a defined density, ranging from 2.5×10^4–6.5×10^4 cells/ml depending on cell line. After 48 h, Herceptin (Genentech, Inc., South San Francisco, CA, USA) was added to the cell cultures at concentrations of 1, 10, 100, and 500 μg/ml. Fresh medium lacking Herceptin was added to control wells of each cell line. After 72 h incubation, the medium was replaced with a fresh drug-free medium and the cells were allowed to recover for additional 18 h. The suppression of cell growth was determined using the alamarBlue Assay (Alamar Biosciences, Sacramento, CA, USA). AlamarBlue was added to the wells in an amount equal to 10% of the total culture medium volume. AlamarBlue was incubated for 4–10 h, and absorbance at 540 and 620 nm wavelengths was measured with a spectrophotometer. The growth suppression of Herceptin-treated vs untreated control cells were calculated according to the manufacturer's instructions (Alamar Biosciences, Sacramento, CA, USA). Mean + 1 s.d. of triplicate experiments are shown

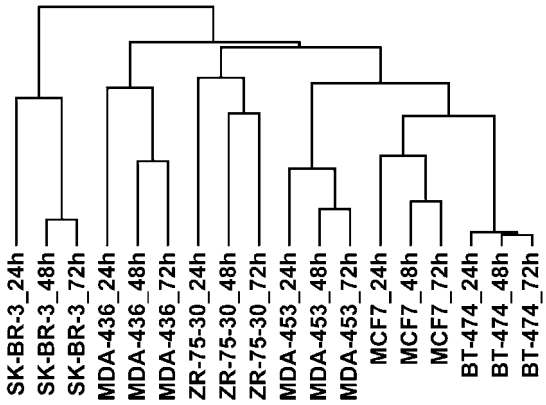

Figure 2 Hierarchical clustering of Herceptin-treated breast cancer cell lines. Cells were cultured in 185 cm^2 flasks and Herceptin was added to exponentially growing cells at a concentration of 10 μg/ml. Control cells were grown in a drug-free medium. Cells were harvested by trypsinization after 24, 48, and 72 h and were washed twice with ice-cold PBS buffer. The cell pellet was snap-frozen in liquid nitrogen and stored at -70°C until RNA isolation. mRNA was extracted using the FastTrack 2.0 mRNA Isolation Kit (Invitrogen, Carlsbad, CA, USA). mRNA (3 μg) from Herceptin-treated cells was labeled with Cy3-dUTP (Amersham Pharmacia Biotech, Piscataway, NJ, USA) and 3 μg of mRNA from untreated control cells of the same cell line was labeled with Cy5-dUTP using oligo(dT)-primed polymerization by SuperScript II reverse transcriptase (Invitrogen, Carlsbad, CA, USA). The preparation and printing of the 14 380-cDNA clones on glass slides and hybridization of labeled cDNAs on microarrays were carried out as described (Mousses *et al*., 2000; Monni *et al*., 2001). The fluorescence intensities at the targets were measured using a laser confocal scanner (Agilent Technologies, Palo Alto, CA, USA) and the data were analysed using the DEARRAY software (Chen *et al*., 1997). After background subtraction, average intensities at each spot in the Herceptin-treated test hybridization were divided by the average intensity of the same spot in the untreated control hybridization. Low-quality measurements (test and reference intensity <100 fluorescent units and/or spot size <50 U) were excluded from the analysis and were treated as missing values. The number of clones that passed the quality filtering was 11 311. The data were normalized using local weighted scatter plot smoother (LOWESS) analysis (Cleveland, 1979; Yang *et al*., 2001) for each print-tip group. The fraction of data points used in local regression (f) was 0.2 and other parameters were adjusted as suggested by Cleveland (1979). Hierarchical clustering of the 11 311 genes at 24, 48, and 72 h time points was performed using the average linkage method with uncentered correlation as the distance function (Eisen *et al*., 1998)

MCF7 cells did illustrate a 20% inhibition with the highest dose used. MDA-436 cells were most resistant and showed a noticeable growth suppression only with 500 μg/ml Herceptin (Figure 1). Similar to the non-amplified cell lines, the MDA-453 cell line with low-level *HER2* amplification showed virtually no response with 1 μg/ml Herceptin. However, a clear growth reduction was observed in MDA-453 cells with higher doses of Herceptin, although with only a small difference between doses of 100 and 500 μg/ml (Figure 1). Overall, the difference in mean growth suppression between the *HER2* amplified (BT-474, SK-BR-3, ZR-75-30, MDA-453) and nonamplified (MCF7, MDA-436) cell line groups was statistically significant ($P<0.05$, two-tailed t-test) with Herceptin doses of 10, 100, and 500 μg/ml.

Next, we explored the specific effects of Herceptin treatment in the *HER2*-amplified and nonamplified breast cancer cell lines using a cDNA microarray containing 14 380 clones. The cells were treated for 24, 48, and 72 h with 10 μg/ml Herceptin, a dose showing a statistically significant difference in growth suppression between the amplified and nonamplified cell lines with a maximum number of viable cells. The expression levels in the treated cells at specific time points were compared to those of untreated cells of the same cell line. Hierarchical clustering was performed to evaluate the overall expression changes caused by Herceptin treatment. For each cell line, the three different time points clustered together indicating that the global expression patterns within a cell line were more similar than those between different samples (Figure 2). Moreover, the hierarchical clustering dendrogram also revealed that for all cell lines the 48 and 72 h time points were more similar to one another than to the 24 h time point (Figure 2). This result suggests that the main effect of Herceptin on transcript levels occurs between 24 and 48 h of drug treatment.

A combination of statistical methods (Hautaniemi *et al*., 2003a) was then used to identify a specific set of genes whose expression levels either increased or decreased as a function of time during Herceptin treatment. First, equalization transformation (Bolstad *et al*., 2003) was performed to obtain a similar range for ratios across the time-series experiments. Linear regression analysis was then applied to convert the three time-series observations to a single number T, where the sign of T reflects the direction of change in the expression

level (either decrease or increase) and the value of T corresponds to the magnitude of expression change. After calculation of the T-values, a stepwise gene selection algorithm was utilized to identify genes that would best separate the *HER2* amplified cell lines from those with no amplification. For this purpose, we assigned the BT-474, SK-BR-3, and ZR-75-30 cell lines as amplified and MDA-436 and MCF7 as nonamplified. MDA-453 was excluded because it did not fit into either category. Genes where the difference in the median expression level between the amplified and nonamplified groups was less than one were excluded, leaving 2990 genes for the analysis. In the stepwise gene selection, the weight (W) for each gene was computed using Fisher's linear discriminant and new genes were added to the set until W reduced to three. As a result, a set of 439 discriminatory genes were identified representing 15% of the genes included in the stepwise gene selection procedure (Supplemental Table 1). Of these, 212 and 227 genes showed decreasing and increasing expression levels, respectively, after the Herceptin treatment in the amplified vs nonamplified cell lines, demonstrating an almost equal partitioning of up- and downregulated discriminatory genes. A randomization test (Hautaniemi *et al*., 2003a) was applied for the 2990 genes to verify that the result was statistically significant ($P<10^{-9}$). The expression level of the *HER2* gene varied less than twofold during the antibody treatment in all cell lines, indicating that the treatment did not have a significant effect on the expression of the *HER2* receptor itself.

Two different clustering approaches were used to illustrate the temporal gene expression changes among the 439 discriminatory genes (Figure 3). In hierarchical clustering, the amplified and nonamplified cell lines were clustered at the opposite ends of the dendrogram. The self-organizing map revealed two major clusters of genes, whose expression profiles were almost opposite in the amplified and nonamplified cell lines. These results demonstrate that the expression profiles of the discriminatory genes were clearly distinct between the *HER2*-amplified and nonamplified cell lines, thereby confirming the validity of the set of discriminatory genes. Interestingly, both clustering methods indicated that the expression changes in the MDA-453 cell line were different from those in the other cell lines with *HER2* amplification, with a large fraction of genes showing temporal gene expression patterns similar to those seen in the nonamplified cell lines. This transcriptional profile might be explained by the fact that the low-level *HER2* amplification in MDA-453 leads only to a slight increase in HER2 expression (Kauraniemi *et al*., 2001; Hyman *et al*., 2002), and therefore the effects of Herceptin treatment in MDA-453 mimic those seen in cells with no *HER2* amplification.

The publicly available gene ontology information (http://source.stanford.edu/cgi-bin/sourceSearch) provided information on the functional roles of 59% of the discriminatory genes. The remaining 179 genes represented hypothetical proteins or known genes with no associated functional information. Closer examination of the gene ontology data revealed that a large

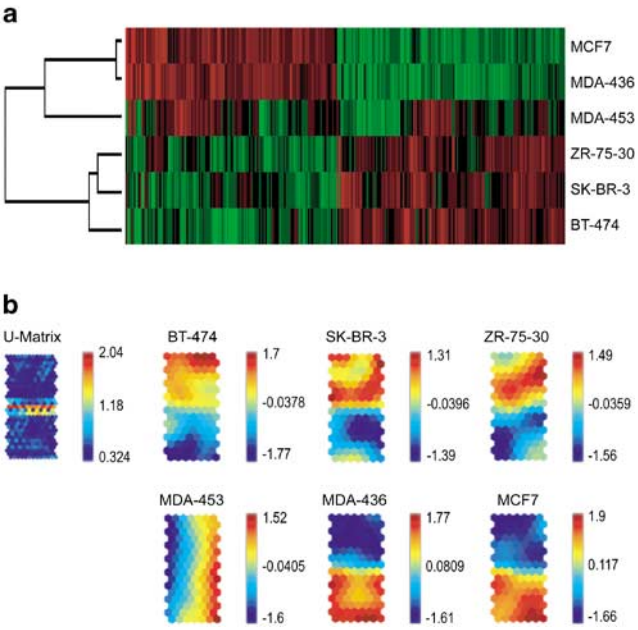

Figure 3 Clustering of the 439 discriminatory genes. (**a**) Hierarchical clustering was performed using the average linkage method with Euclidean distance as the distance function. Changes in the expression levels (T-values) are illustrated using a color-coding, where red corresponds to increasing expression levels, green to decreasing expression level, and black to stable expression during the time series. (**b**) Clustering of the 439 genes was performed using the SOM algorithm (Kohonen, 2001; Hautaniemi *et al*., 2003b) using a toolbox made by Vesanto *et al*. (2000). The unified-distance matrix (U-matrix) and component plane representation are shown. The U-matrix illustrates the presence of two major clusters of genes (shown in blue) that are separated by a row of red-shaded map units. The colored component planes for each cell line indicate that the expression patterns of these major clusters in the amplified cell lines are markedly different from those seen in the nonamplified cell lines. In the component planes, the expression patterns are illustrated using a specific color scheme, where shades of red correspond to increase in expression, shades of yellow to stable expression, and shades of blue to decrease in expression during the time series

number of the discriminatory genes encode for proteins involved in key cellular processes like transcription, signal transduction, protein processing, cell metabolism, and transport. Genes encoding proteins involved in various RNA processing reactions, for example, biogenesis of spliceosomal snRNAs (*SIP1*), RNA 3′-end processing (*CPSF4*), and nuclear pre-mRNA splicing (*PRPF31*) were upregulated by Herceptin treatment in the amplified cell lines. Herceptin treatment also induced the expression of genes involved in various DNA repair pathways, for example, nucleotide-excision (*ERCC2*), double-strand break (*MRE11*), and DNA mismatch repair (*MSH5*). On the other hand, genes encoding cell adhesion proteins (e.g. *JUP*, *CTNND2*, and *CNTN1*) or well-characterized oncoproteins (e.g. *FOS* and *KIT*) showed decreasing expression levels in the amplified cell lines during the drug treatment. Several studies have shown that estrogen-induced mitogenesis of breast cancer cells is partly mediated by the increased expression of c-FOS, indicating an important role for *c-FOS* in

breast cancer pathogenesis (Wilding *et al*., 1988; Van der Burg *et al*., 1989; Duan *et al*., 2002). Although *c-KIT* oncogene, encoding a transmembrane receptor tyrosine kinase, has not been previously implicated in breast cancer, it is often activated in a number of human malignancies, including mast cell leukemia (Furitsu *et al*., 1993), acute myeloid leukemia (Longley *et al*., 2001), and gastrointestinal stromal tumors (Hirota *et al*., 1998).

In conclusion, the Herceptin treatment induced a dose-dependent growth reduction in *HER2* amplified breast cancer cell lines. The expression profiling identified a set of 439 genes whose temporal expression patterns discriminated between the amplified and nonamplified cell lines. These included several genes involved in key cellular processes, such as RNA processing, DNA repair, cell adhesion, and oncogenesis. Detailed analysis of these genes is likely to provide additional information on the downstream effects of blocking the *HER2* pathway in breast cancer.

Acknowledgements
We thank Ms Kati Rouhento for excellent technical assistance. This work was supported by the Academy of Finland, Foundation for Finnish Cancer Institute, the Medical Research Fund of the Tampere University Hospital, the Science Fund of Tampere, as well as Finnish and Pirkanmaa Cultural Foundations.

References

Baselga J, Tripathy D, Mendelsohn J, Baughman S, Benz CC, Dantis L, Sklarin NT, Seidman AD, Hudis CA, Moore J, Rosen PP, Twaddell T, Henderson IC and Norton L. (1996). *J. Clin. Oncol.,* **14,** 737–744.

Bolstad B, Irizarry R, Astrand M and Speed TA. (2003). *Bioinformatics,* **19,** 185–193.

Carter P, Presta L, Gorman CM, Ridgway JB, Henner D, Wong WL, Rowland AM, Kotts C, Carver ME and Shepard HM. (1992). *Proc. Natl. Acad. Sci. USA,* **89,** 4285–4289.

Chen Y, Dougherty ER and Bittner ML. (1997). *J. Biomed. Optics,* **2,** 364–374.

Cleveland W. (1979). *J. Am. Stat. Assoc.,* **74,** 829–836.

Cobleigh MA, Vogel CL, Tripathy D, Robert NJ, Scholl S, Fehrenbacher L, Wolter JM, Paton V, Shak S, Lieberman G and Slamon DJ. (1999). *J. Clin. Oncol.,* **17,** 2639–2648.

Duan R, Xie W, Li X, McDougal A and Safe S. (2002). *Biochem. Biophys. Res. Commun.,* **294,** 384–394.

Eisen M, Spellman P, Brown P and Botstein D. (1998). *Proc. Natl. Acad. Sci. USA,* **95,** 14863–14868.

Furitsu T, Tsujimura T, Tono T, Ikeda H, Kitayama H, Koshimizu U, Sugahara H, Butterfield JH, Ashman LK, Kanayama Y, Matsuzawa Y, Kitamura Y and Kanakura Y. (1993). *J. Clin. Invest.,* **92,** 1736–1744.

Hautaniemi S, Kauraniemi P, Rämö P, Yli-Harja O, Astola J and Kallioniemi A. (2003a). *A Strategy for Identifying Class-Separating Genes in Drug-Treatment Microarray Data. Report 1*. Institute of Signal Processing, Tampere University of Technology: Finland, ISBN 952-15-1067-6..

Hautaniemi S, Yli-Harja O, Astola J, Kauraniemi P, Kallioniemi A, Wolf M, Ruiz J, Mousses S and Kallioniemi O-P. (2003b). *Mach. Learn.,* **52,** 45–66.

Hirota S, Isozaki K, Moriyama Y, Hashimoto K, Nishida T, Ishiguro S, Kawano K, Hanada M, Kurata A, Takeda M, Muhammad Tunio G, Matsuzawa Y, Kanakura Y, Shinomura Y and Kitamura Y. (1998). *Science,* **279,** 577–580.

Hyman E, Kauraniemi P, Hautaniemi S, Wolf M, Mousses S, Rozenblum E, Ringner M, Sauter G, Monni O, Elkahloun A, Kallioniemi OP and Kallioniemi A. (2002). *Cancer Res.,* **62,** 6240–6245.

Kauraniemi P, Bärlund M, Monni O and Kallioniemi A. (2001). *Cancer Res.,* **61,** 8235–8240.

Kohonen T (ed). (2001). *Self-Organizing Maps*, 3rd edn Springer: Heidelberg, Germany.

Longley BJ, Reguera MJ and Ma Y. (2001). *Leuk. Res.,* **25,** 571–576.

Molina MA, Codony-Servat J, Albanell J, Rojo F, Arribas J and Baselga J. (2001). *Cancer Res.,* **61,** 4744–4749.

Monni O, Bärlund M, Mousses S, Kononen J, Sauter G, Heiskanen M, Paavola P, Avela K, Chen Y, Bittner ML and Kallioniemi A. (2001). *Proc. Natl. Acad. Sci. USA,* **98,** 5711–5716.

Mousses S, Bittner ML, Chen Y, Dougherty ER, Baxevanis A, Meltzer PS and Trent JM. (2000). *Functional Genomics: Gene Expression Analysis by cDNA Microarrays*, Livesey FJ and Hunt SP (eds). Oxford University Press: Oxford, pp. 113–137.

Ross JS and Fletcher JA. (1999). *Semin. Cancer Biol.,* **9,** 125–138.

Slamon DJ, Leyland-Jones B, Shak S, Fuchs H, Paton V, Bajamonde A, Fleming T, Eiermann W, Wolter J, Pegram M, Baselga J and Norton L. (2001). *N. Engl. J. Med.,* **344,** 783–792.

van der Burg B, van Selm-Miltenburg AJ, de Laat SW and van Zoelen EJ. (1989). *Mol. Cell. Endocrinol.,* **64,** 223–228.

Vesanto J, Himberg J, Alhoniemi E and Parhankangas J. (2000). *SOM Toolbox for Matlab 5. Technical Report A57*. Helsinki University of Technology: Finland.

Vogel CL, Cobleigh MA, Tripathy D, Gutheil JC, Harris LN, Fehrenbacher L, Slamon DJ, Murphy M, Novotny WF, Burchmore M, Shak S, Stewart SJ and Press M. (2002). *J. Clin. Oncol.,* **20,** 719–726.

Wilding G, Lippman ME and Gelmann EP. (1988). *Cancer Res.,* **48,** 802–805.

Yakes FM, Chinratanalab W, Ritter CA, King W, Seelig S and Arteaga CL. (2002). *Cancer Res.,* **62,** 4132–4141.

Yang Y, Dudoit S, Luu P and Speed T. (2001). *Microarrays: Optical Technologies and Informatics*, Bittner M, Chen Y, Dorsel A and Dougherty E (eds). SPIE, Society for Optical Engineering: San Jose, CA, pp. 141–152.